International Journal of Earth Sciences (2025) 114:825–840
https://doi.org/10.1007/s00531-025-02521-2

ORIGINAL PAPER

# Top-to-the-S vs top-to-the-N extensional shearing in the southern Cyclades, Aegean Sea, Greece: new geochronologic data

**Uwe Ring**[1] · **Johannes Glodny**[2] · **Alexandre Peillod**[1,3]

Received: 15 April 2025 / Accepted: 30 June 2025 / Published online: 15 July 2025


## Abstract

The geometry of large-scale extensional deformation in the southwestern Cyclades archipelago is a controversially discussed issue. Recent studies suggest a bivergent (i.e., coeval top-to-the-S and top-to-the-N shear) geometry of early Miocene extensional deformation. On Sikinos Island, top-to-the-S shear structures in the Cycladic basement are overprinted by a prominent ductile-to-brittle top-to-the-N extensional shear zone in the Cycladic basement at its contact with the tectonically overlying passive-margin sequence of the Cycladic Blueschist Unit. Hitherto, the top-to-the-S shear structures have been related to thrusting of the passive-margin sequence onto the Cycladic basement. Rb–Sr multimineral dating constrains the age of retrograde, lower greenschist-facies top-to-the-S shearing at 23.20 ± 0.25 Ma. This age is identical to published $^{40}Ar/^{39}Ar$ ages of ~ 23 Ma for a lower greenschist-facies top-to-the-S extensional shear zone on nearby Folegandros Island. Therefore, an interpretation of the top-to-the-S shear zone in the Cycladic basement of Sikinos as resulting from extensional deformation is consistent with the regional scale context of crustal extension invoked for the Cyclades in the early Miocene. On Folegandros Island, top-to-the-S extension occurs at the top of the passive-margin sequence of the Cycladic Blueschist Unit, whereas on Sikinos coeval top-to-the-S extension occurs near the top of the underlying Cycladic basement. Our new Rb–Sr age of ~ 23 Ma indicates that top-to-the-S fabrics reflect the earliest Miocene extensional structures. They are intimately related to the top-to-the-N extensional structures forming an early Miocene bivergent extensional hinge zone at the southern end of the Cyclades archipelago.

**Keywords** Structural mapping · Rb–Sr geochronology · Extensional deformation · Cycladic Blueschist Unit · Sikinos Island · Cyclades · Greece

## Introduction

The Cyclades archipelago in the central Aegean Sea (Fig. 1) is a remarkable example of large-scale lithospheric extension above the retreating Hellenic subduction zone (Jolivet and Brun 2010; Ring et al. 2010; Grasemann et al. 2012) since the early Miocene (~ 23 Ma) (Büttner and Kowalczyk 1978; Kuhlemann et al. 2004; Glodny and Ring 2022; Bakowsky et al. 2023). At the northern periphery and in the central Cyclades, the geometry of extension is distinctly asymmetric with a top-to-the-N shear sense resolved on ductile and ductile-to-brittle extensional shear zones (Avigad and Garfunkel 1991; Lee and Lister 1992; Gautier and Brun 1994; Ring et al. 2003; Kumerics et al. 2005; Brichau et al. 2006, 2007, 2010; Jolivet et al. 2010) (Fig. 1, 2).

In the southwestern Cyclades, the geometry of extensional deformation is more complicated. Ring et al. (2011) studied top-to-the-S extensional shear zones within the lower parts of the Cycladic Blueschist Unit (CBU), mainly between its passive-margin sequence and the contact to the underlying basement, and summarized the structures as the South Cycladic Detachment. Subsequently, Grasemann et al. (2012) lumped top-to-the-S extensional structures near the top of the CBU and its contact with overlying tectonic units (Fig. 2) as the West Cyclades Detachment. All these detachments are typical core-complex-style structures (cf. Lister and Davis 1989) characterized by mylonitic deformation in

✉ Uwe Ring
uwe.ring@geo.su.se

[1] Department of Geological Sciences, Stockholm University, 10691 Stockholm, Sweden

[2] German Research Centre for Geosciences (GFZ), 14473 Potsdam, Germany

[3] Chair of Geochemistry & Economic Geology, Karlsruhe Institute of Technology (KIT), Karlsruhe, Germany

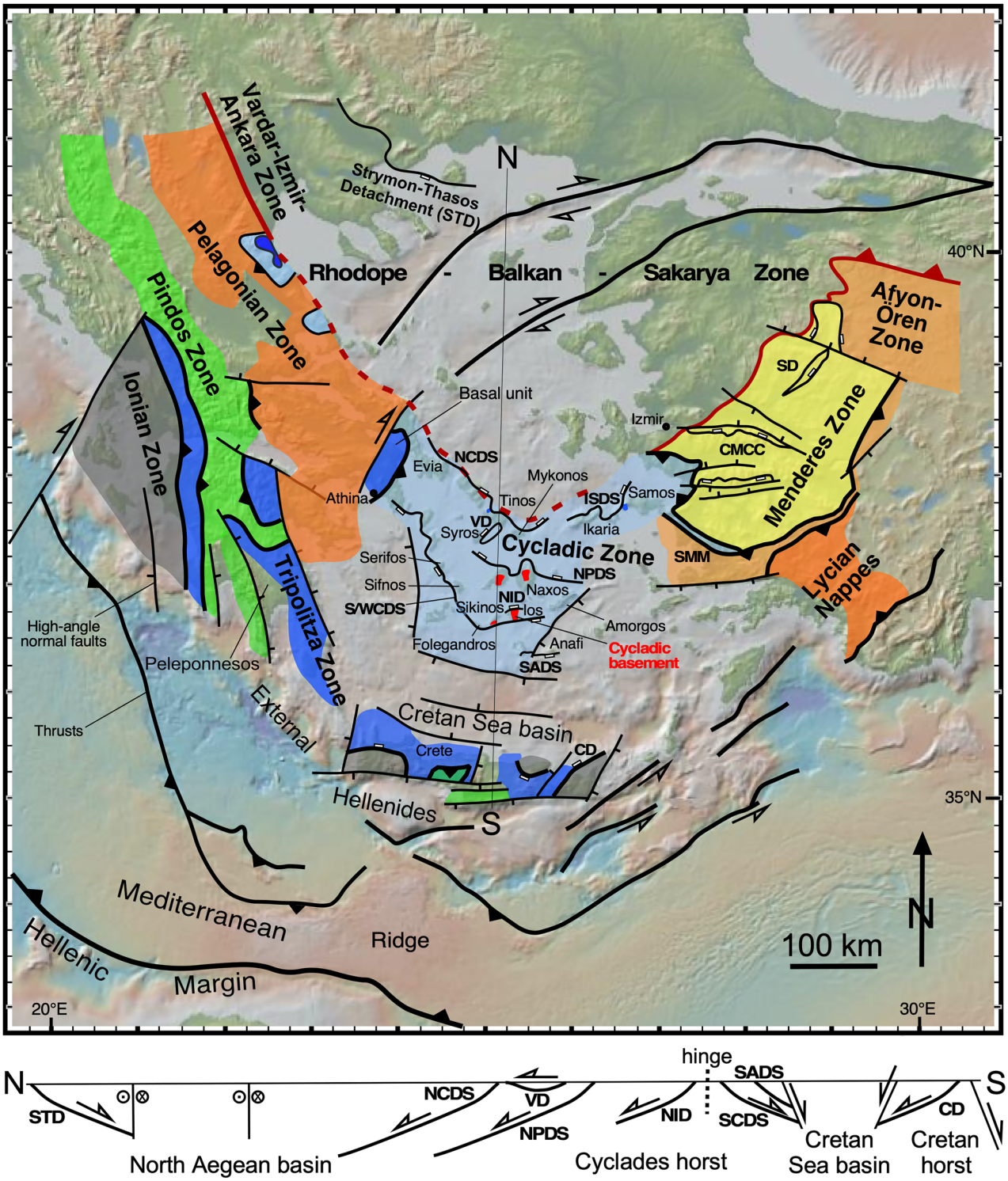


**Fig. 1** Aegean tectonic map with major tectonic zones and cross section with major extensional detachment systems. The simplified cross section shows the basin and horst structure of Aegean, which at the Aegean-wide scale appears rather symmetric, with the asymmetric Cyclades horst being dominated by top-N extensional detachments. Also shown are outcrops of the Cycladic basement (red) in the central and southern Cyclades (note that the basement on Naxos is disputed, see text). *NCDS* North Cyclades Detachment System, *ISDS* Ikaria-Samos Detachment System, *NPDS* Naxos-Paros Detachment System, *VD* Vari Detachment, *NID* North Ios Detachment, *S/WCDS* South/West Cyclades Detachment System, *SADS* Santorini-Anafi Detachment System, *CD* Cretan Detachment, *SDF* Simav Detachment, *CMCC* Central Menderes metamorphic core complex, *SMM* South Menderes Monocline. Base map from GeoMapApp (http://www.geomapapp.org) (Ryan et al. 2009)

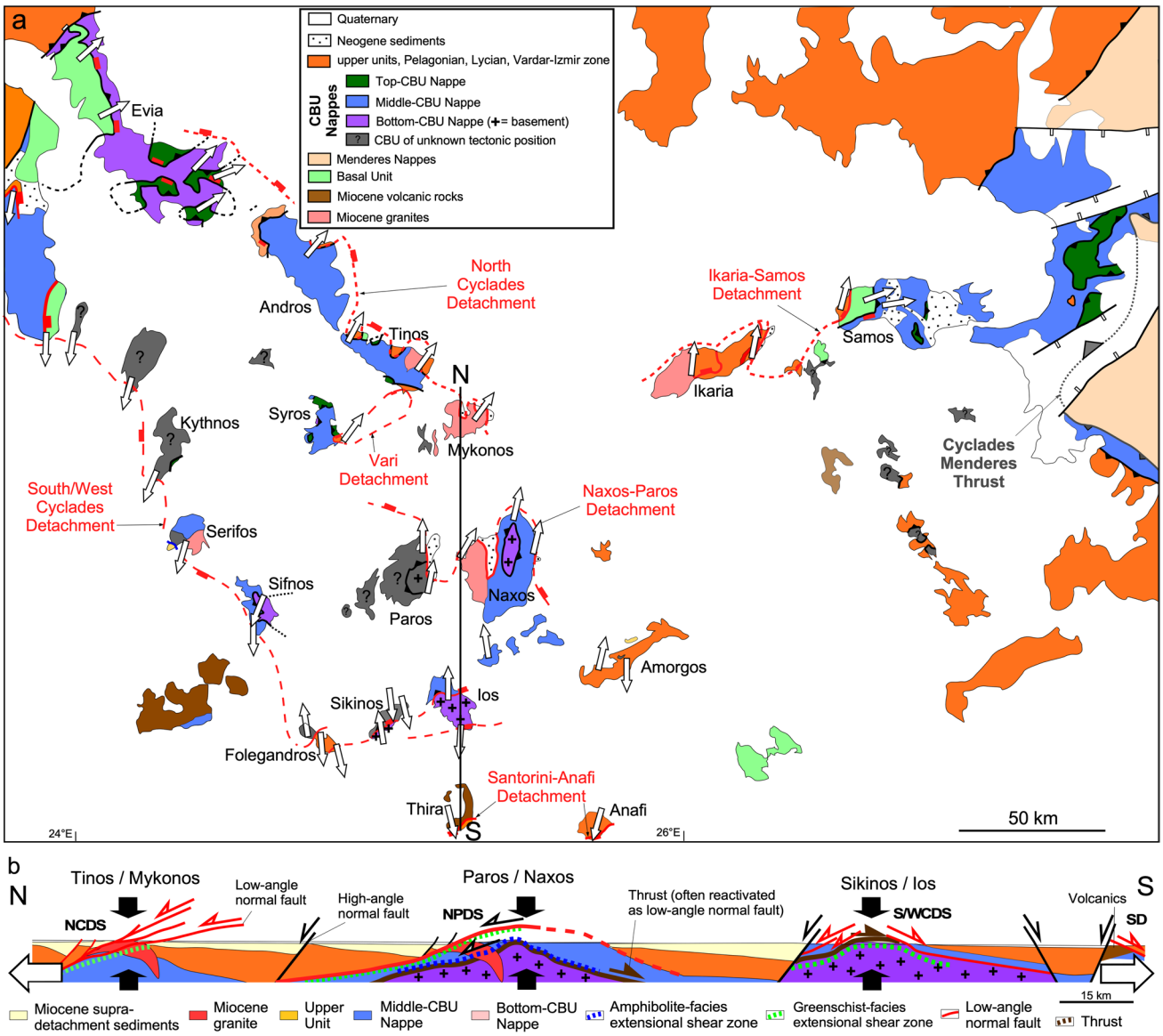


**Fig. 2** Tectonic map and cross section of the Cyclades. **a** The tectonic map displays the subdivision of the Cycladic Blueschist Unit into the Top-, Middle- and Bottom-CBU nappes. The main extensional detachments (i.e., extensional ductile shear zones overlain by subgreenschist-facies to brittle low-angle normal faults) are also shown. The open arrows in the map indicate the movement directions of the upper plate of the extensional detachments according to Augier et al. (2015), Avigad and Garfunkel (1989, 1991), Bakowsky et al. (2023), Beaudoin et al. (2015), Coleman et al. (2020), Ducharme et al. (2022), Grasemann et al. (2012), Jolivet et al. (2010), Kumerics et al. (2005), Laskari et al. (2022, 2024), Lee and Lister (1992), Ring and Layer (2003), Ring et al. (2011, 2003), Rosenbaum et al. (2007), Scheffer et al. (2016), Schneider et al. (2018), Soukis and Papanikolaou (2004), Thomson et al. (2009) and Vandenberg and Lister (1996). **b** The cross section illustrates the asymmetry of the Cyclades horst as expressed by the prominent top-N extensional detachments, and that the extensional structures are subparallel to the earlier thrusts. The bold vertical arrows show that the extensional structures are associated with a distinct component of vertical shortening. Abbreviations as in Fig. 1, except VIA in the legend = Vardar–Izmir–Ankara

a broad, ductile shear zone grading structurally upward into subgreenschist-facies to cataclastic deformation directly below the extensional detachment.

Despite the dominance of top-to-the-S extensional shearing in the southern and western Cyclades, there is debate on the tectonic significance of top-to-the-N vs top-to-the-S kinematic indicators. The island of Ios (Fig. 2) serves as an example to highlight the different views. Vandenberg and Lister (1996) suggested initial top-to-the-N extension followed by dominant top-to-the-S extensional shear, the latter mainly being accommodated by the South Cyclades Shear Zone/Ios Detachment at the

south end of Ios (Vandenberg and Lister 1996; Thomson et al. 2009; Mizera and Behrmann 2016). Huet et al. (2009) claimed that top-to-the-S shear is related to thrusting, not extension, and that the latter was exclusively top-to-the-N directed. Thomson et al. (2009) took this discussion a step further by directly dating deformation structures. Their data indicate that top-to-the-S and top-to-the-N ductile extension were largely coeval at 18 ± 1 Ma. A finite-strain study by Mizera and Behrmann (2016) in the joint footwall of both extensional systems also concluded that extension has a bivergent (i.e., coeval top-to-the-S and top-to-the-N shear) deformation geometry and was characterized by a distinct component of vertical shortening.

Radiometric dating of top-to-the-N and top-to-the-S deformation fabrics might help to shed more light on the tectonic significance of the shear-sense indicators. In line with this, Bakowsky et al. (2023) studied lower greenschist-facies (< 415–395 °C) top-to-the-S extensional structures between the CBU in the footwall and the Pelagonian Zone in the hanging wall, the Folegandros Detachment (Fig. 2). $^{40}Ar/^{39}Ar$ white-mica ages were interpreted to date the onset of top-to-the-S extension at ~ 23 Ma. Bakowsky et al. (2023) also mapped top-to-the-N extensional structures and inferred that they overprinted the top-to-the-S structures (their Fig. 9). On Sikinos Island between Folegandros and Ios, Ring and Glodny (2021) similarly reported top-to-the-N and top-to-the-S extensional structures in the Cycladic Blueschist Unit and suggested that they formed largely coevally during pronounced extension-related flattening deformation. Ring and Glodny (2021) proposed that bivergent extension defines an extensional hinge zone, i.e., a joint footwall of a bivergent low-angle extensional fault system, that resulted in up to ~ 40% of vertical shortening, an amount that is similar to that reported by Mizera and Behrmann (2016) from Ios Island.

In this article, we revisited top-to-the-S and top-to-the-N shear-sense indicators at the contact between the basement and the tectonically overlying passive-margin sequence of the CBU on Sikinos Island. The top-to-the-S structures were hitherto understood to be due to thrusting (Gupta and Bickle 2004; Augier et al. 2015; Ring and Glodny 2021). However, the top-to-the-S structures did not all form at the same metamorphic grade. This is evidenced in the field by garnets, which are either pristine in asymmetric deformation structures or show different degrees of chloritization. In the Cyclades, asymmetric strain shadows around chloritized (i.e., destabilizing) garnet forming at lower greenschist-facies conditions (< ~ 390–350 °C) (e.g., Kleine et al. 2014; see also Peillod et al. 2017, 2021a, b; Laurent et al. 2018) are typically related to extensional shearing. We dated one of the retrogressive top-to-the-S structures by the Rb–Sr method and discuss implications of the age data for the geometry of extensional deformation in the southern Cyclades.

## Setting

### Hellenide orogen

The Hellenides are an arcuate orogen stretching from mainland Greece across the Aegean Sea into western Turkey (Fig. 1). They formed, and still form, to the north of the Hellenic trench, along which NNE-ward subduction of the African plate beneath Eurasia is accommodated. The Aegean Sea transect of the Hellenide orogen has been shaped by the retreat of the Hellenic subduction zone (e.g., Jolivet et al. 2015).

The general architecture of the Hellenides in Greece reveals that the tectonic units are north dipping, i.e., the orogen youngs southward and can be subdivided from top (north) to bottom (south) into: (1) The Rhodope–Balkan–Sakarya Zone, (2) the Vardar–Izmir–Ankara Zone, (3) the Pelagonian–Lycian Zone, (4) the Cycladic Zone, and (5) the External Hellenides (incl. the Pindos, Tripolitza and Ionian zones) (Dürr et al. 1978; Jacobshagen et al. 1986) (Fig. 1). The Cycladic Zone is important for this article.

The dominant rock unit of the Cycladic Zone is the CBU (Fig. 2), which represents stretched continental fragments of the Adriatic Plate. The major lithotectonic members of the CBU are in structurally descending order: (i) A mélange-like assemblage of ophiolitic rocks and garnet-mica schist embedded in a serpentinitic chlorite-talc schist matrix (Okrusch and Bröcker 1990; Ring et al. 1999; Bröcker et al. 2014). (ii) A Permo-Carboniferous to latest Cretaceous passive-margin sequence composed of marble, metapelite, quartzite and metabasite. The bottom parts of this section have been intruded by Triassic granitoids (Reischmann 1998; Ring et al. 1999; Poulaki et al. 2019). (iii) An early Paleozoic to Carboniferous (Cycladic) basement (Reischmann 1998; Flansburg et al. 2019), consisting mainly of orthogneiss and garnet-mica schist (Ring et al. 1999) (Fig. 2). A review of geochronologic data by Glodny and Ring (2022) showed that these three lithotectonic units are imbricated with each other and define the Top- Middle- and Bottom-CBU nappes. The Top-CBU Nappe (which includes the ophiolites) was accreted first at ~ 55–45 Ma. The Top-CBU Nappe was exhumed in an extrusion wedge while the underlying Middle-CBU-Nappe was underthrust and high-pressure (P) metamorphosed at ~ 45–34 Ma. Subsequently, the Bottom-CBU Nappe (which includes the Cycladic basement) was underthrust and underwent high-P metamorphism at ~ 34–28 Ma, while the Middle-CBU nappe was exhumed (Peillod et al. 2024). The close proximity of underthrusting of one CBU nappe and the exhumation of the overlying one

in extrusion wedges shows that the contacts between the nappes were early thrusts that were reactivated as a low-angle normal shear zones (cf. Glodny and Ring 2022).

The Cycladic basement as part of the Bottom-CBU Nappe experienced lower-grade high-P metamorphism than the CBU passive-margin sequence above (Franz et al. 1993; Gupta and Bickle 2004; van der Maar and Jansen 1983; Grütter 1993). Because the high-P rocks of the passive-margin sequence are tectonically above the lower-grade high-P rocks of the Cycladic basement, the contact must have been an early thrust (Huet et al. 2009; Peillod et al. 2017) that was reactivated in many places by top-to-the-N and top-to-the-S extensional shearing (Vandenberg and Lister 1996; Thomson et al. 2009; Augier et al. 2015) resulting from subduction-zone retreat (Jolivet et al. 2010; Ring et al. 2010). An alternative view by Vanderhaeghe (2004), Vanderhaeghe et al. (2007), Martin et al. (2006) and Scheffer et al. (2016) envisages that thermal relaxation of orogenic crust following high-P metamorphism transposed (and not reworked) the CBU during exhumation, the latter of which was related to gravitational collapse.

The CBU in the footwalls of the Cycladic extensional detachments was intruded by S- and I-type plutons between ~ 17 and ~ 11 Ma (Altherr et al. 1982; Bolhar et al. 2010, 2012; Lamont et al. 2023) during a regionally widespread greenschist-/amphibolite-facies metamorphic event at ~ 23–11 Ma (Wijbrans and McDougall 1988; Bröcker et al. 1993, 2013; Kumerics et al. 2005; Cao et al. 2017; Beaudoin et al. 2015; Bolhar et al. 2017; Ring et al. 2018). Supra-detachment sediment deposition above the CBU commenced in the early Miocene (Angelier et al. 1978; Büttner and Kowalczyk 1978; Rösler 1978; Dermitzakis et al. 1980; Böger 1983; Sánchez-Gómez et al. 2002; Kuhlemann et al. 2004).

## Geology of Sikinos Island

Sikinos Island is entirely made up of rocks of the CBU, encompassing the Cycladic basement tectonically overlain by the passive-margin sequence (van der Maar 1981; van der Maar and Jansen 1983; Franz et al. 1993; Avdis and Photiades 1999; Gupta and Bickle 2004; Augier et al. 2015) (Fig. 3). The boundary between the two units may coincide with the Middle-/Bottom-CBU nappe contact, but there are no geochronologic data that would support this proposition.

The pre-Permian basement consists of granodioritic gneiss and metaaplitic dikes, metavolcanics (mainly metamorphosed quartz porphyry), garnet-mica schist and rare amphibolite (van der Maar and Jansen 1983; Andriessen et al. 1987; Franz et al. 1993). The basement rocks are polymetamorphic with Carboniferous metamorphism, and an early Tertiary mild high-P stage at 10–12 kbar and 480 ± 20 °C followed by near-isothermal decompression and a greenschist-facies overprint at ≥ 5 kbar and 440–480 °C (van der Maar and Jansen 1983; Andriessen et al. 1987; Franz et al. 1993; Gupta and Bickle 2004) (Fig. 4). The 6–7 km thick passive-margin sequence comprises calcitic

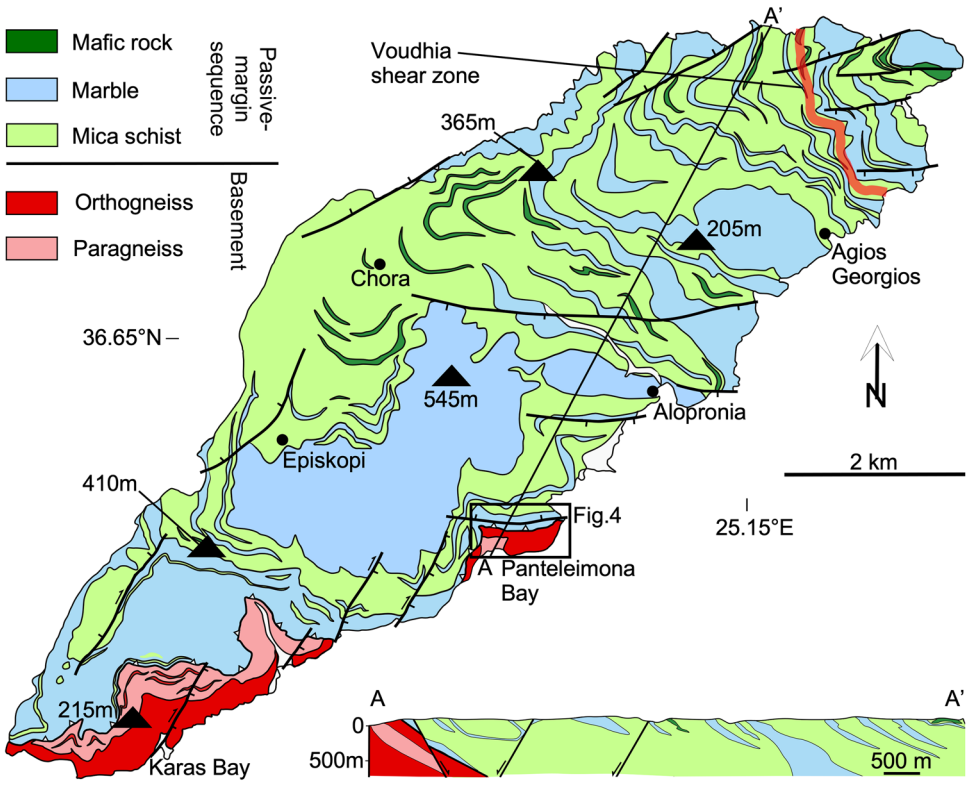


**Fig. 3** Geologic-tectonic map of Sikinos Island with generalized NE–SW cross section. The white triangles above the basement outcrops indicate the basal thrust of the passive-margin sequence onto the basement. The map shows the localities used in the text, the approximate trace of the Voudhia shear zone (orange line) and the position of Fig. 4 (adapted from Augier et al. 2015)

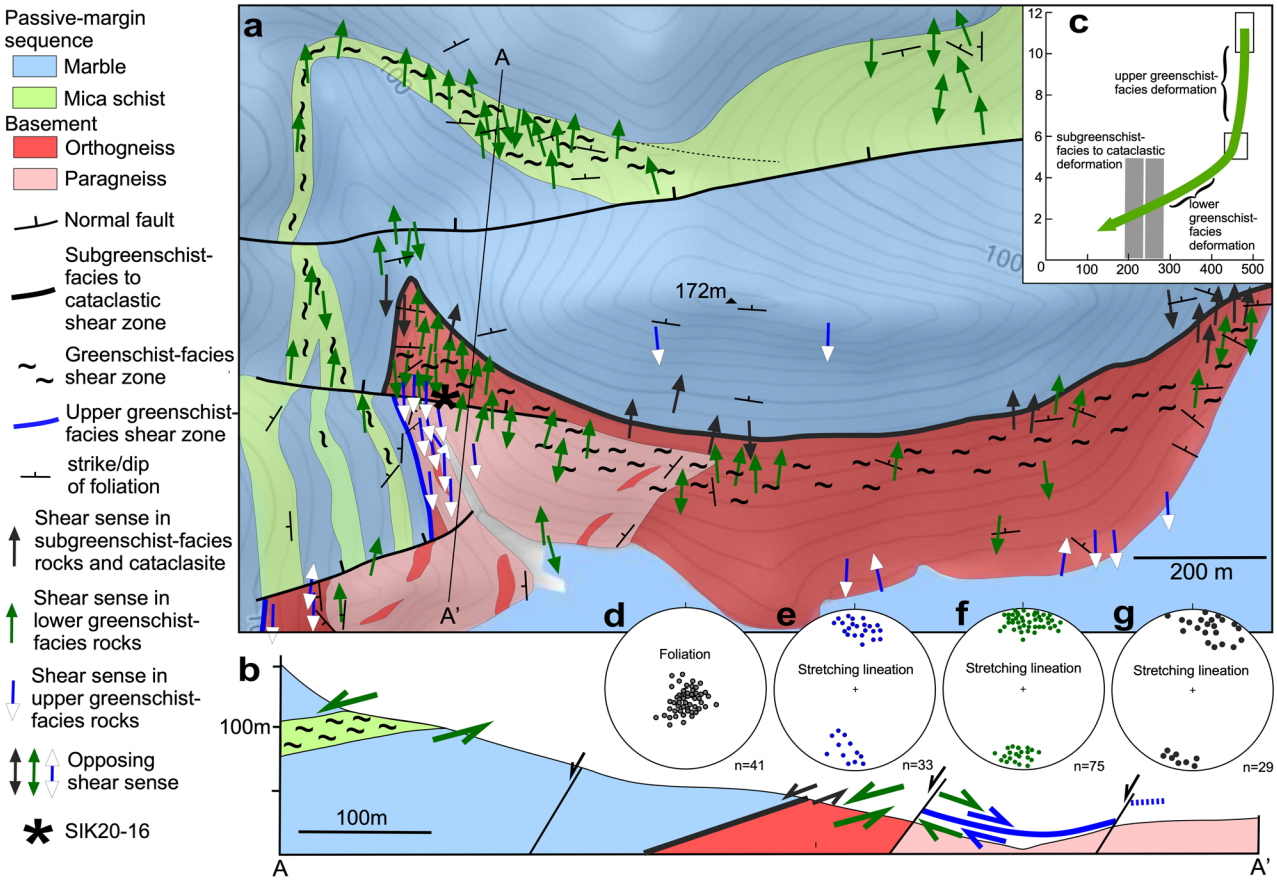


**Fig. 4** Geologic/tectonic map with N–S cross section of the basement/passive-margin sequence contact at Panteleimona Bay. **a** The map shows the main greenschist-facies top-N shear zone in granitic gneiss and garnet-mica schist of the basement and subgreenschist-facies to cataclastic deformation at top of the basement (black line), and another prominent top-N shear zone in quartz-chlorite-albite-mica schist of the passive-margin sequence in the NW. Also shown is an older top-S shear zone at the basement/passive-margin sequence contact in the W (blue line). The locality of the dated sample SIK20-16 (36°39′39″N, 27°07′18″E) is shown by a bold, black star (modified from Ring and Glodny 2021). Note that SIK20-16 is a garnet-mica schist lens in orthogneiss. **b** The N-S cross section illustrates top-S and top-N shear zones in the basement. Near the basement/passive-margin sequence contact, the top-N shear zone overprints a top-S one. **c** P–T diagram for the Cycladic basement based on data of Franz et al. (1993) and Gupta and Bickle (2004) showing approximate metamorphic conditions of the upper and lower greenschist-facies deformation structures. **d**–**g** Lower-hemisphere stereographic projections of the main foliation and stretching lineations in upper, lower, and subgreenschist-facies to cataclastic rocks

and dolomitic marble, and quartz-albite-mica schist with intercalated metabasite lenses (eclogite, blueschist and greenschist) with peak P–T conditions of 16–20 kbar and 480–540 °C) (Augier et al. 2015).

The contact between the Cycladic basement and the overlying passive-margin sequence is a matter of debate. At both exposures of the basement (Fig. 3), up to ~ 300 m of variably deformed granitic gneiss, metavolcanics, paragneiss and garnet-mica schist are overlain by marble (Franz et al. 1993; Avdis and Photiades 1999; Gupta and Bickle 2004; Augier et al. 2015). Detrital zircon U–Pb data of samples collected from the basement and the passive-margin sequence were interpreted to suggest a continuous chronostratigraphic succession across the contact from the basement to the overlying Permo-Triassic clastic passive-margin sequence strata with no evidence for apparent tectonic breaks across the contact (Poulaki et al. 2019).

In contrast, the currently available P–T data suggest a distinct break in the metamorphic grade across the contact. Despite the fact that different methods have been used for obtaining P–T estimates, Franz et al. (1993) and Gupta and Bickle (2004) arrived at very similar P–T estimates for Alpine high-P metamorphism of the basement. Especially, the P estimates show vastly different values for the basement and the overlying passive-margin sequence. A distinct metamorphic break and a broad zone of mylonitically deformed rocks at the contact between the basement and the passive-margin sequence led Gupta and Bickle (2004) and Augier et al. (2015) to argue for significant displacement between the basement and passive-margin sequence, a

view we support (see discussion in Ring and Glodny 2021). Accordingly, the contact putting the higher-grade rocks of the passive-margin sequence onto the lower-grade basement would be a thrust. Assuming a 30° dip angle for this thrust and an average rock density of 2700 kg $m^{-3}$, the P data suggest a displacement of ~ 35–75 km. This large-magnitude displacement would support a Middle-/Bottom-CBU nappe contact.

## Methods

For better understanding structural relationships between top-to-the-S and top-to-the-N sense-of-shear indicators in the Cycladic basement and its contact with the overlying passive-margin sequence, outcrops at Panteleimona Bay were revisited. We also collected sample SIK20-16 from a top-to-the-S shear zone in the Cycladic basement for radiometric dating. We employ the Rb–Sr internal-mineral-isochron approach for isotopic dating of metamorphic mineral growth during ductile deformation/recrystallization. Details of the method are outlined in the accompanying Online Resource and follow Glodny et al. (2008a) and Glodny and Ring (2022). The Rb–Sr system of white mica is thermally stable to temperatures > 600 °C for timescales > 10 Ma at static, fluid-deficient conditions (Glodny et al. 2008a, b). Peak metamorphic temperatures in the CBU are generally below 600 °C (Laurent et al. 2018 and references therein), indicating that white mica in the lithologies crystallized at temperatures insufficient to activate thermal diffusional resetting of Rb–Sr ages (see also Cliff et al. 2017). Hence, white-mica-based Rb–Sr mineral ages either represent crystallization ages or were controlled by deformation or fluid-induced metamorphic recrystallization.

## Results

### Structural mapping across the basement/passive-margin sequence contact

At Panteleimona Bay the structural sequence is north dipping (Figs. 4 a-b, 5a). Garnet-mica schist constitutes the bottom of the basement outcrop and is imbricated with, and overlain by, granitic gneiss. The top of the basement is a ductile shear zone that becomes structurally upwards distinctly brittle in character and forms a prominent subgreenschist-facies to cataclastic shear zone (Franz et al. 1993; Gupta and Bickle 2004; Augier et al. 2015).

Where the basement/passive-margin sequence contact is about N-S striking, a first set of structures is preserved (Fig. 4a) (Gupta and Bickle 2004; Augier et al. 2015; Ring and Glodny 2021). Garnet in these structures does not show any chloritization and asymmetric strain shadows contain white mica and quartz. Potassium feldspar in the foliation planes in granitic gneiss is recrystallized implying $T \geq 450$ °C (Pryer 1993). These structures affect all rock types, including metaaplitic dikes and the metavolcanics. The latter do not show any evidence of the Variscan metamorphic overprint reported by van der Maar (1981) and Franz et al. (1993) suggesting that these structures are Tertiary in age and probably formed close to or slightly after the reported P–T maximum of 10–12 kbar and $480 \pm 20$ °C (Fig. 4c). As we do not have control over metamorphic pressure in the field, we refer to these structures as structures in upper greenschist-facies rocks in Fig. 4. On a variably oriented foliation (Fig. 4d), a N-S-trending stretching lineation developed (Fig. 4e). Asymmetric lozenges of less-deformed rock, S-C structures and asymmetric strain shadows around plagioclase and garnet provide a top-to-the-S sense of shear (Figs. 5b, 6a–c) (see also Gupta and Bickle 2004).

There is a second set of shear-sense indicators associated with partially to strongly chloritized garnet, referred to as structures in lower greenschist-facies rocks in Fig. 4. The shear sense is also top-to-the-S, but the strain shadows include chlorite in addition to white mica, albite and quartz. Potassium feldspar and plagioclase do not recrystallize in the retrograde top-to-the-S structures. Despite the variable retrograde overprint, the orientation of the foliation and the associated stretching lineation remains the same. Because the shear-sense indicators formed during retrograde metamorphism, they must have formed after the first set of upper greenschist-facies structures; however, no overprinting relationships have been observed. Gupta and Bickle (2004) reported late chlorite-filled shear bands at low angles to the main foliation and inferred that they developed during exhumation. Some outcrops show coeval top-to-the-S and top-to-the-N shear-sense indicators (e.g., Fig. 9d in Ring and Glodny 2021).

North and especially east of the N-S striking basement/passive-margin sequence contact, the basement rocks form a 70–80 m thick mylonitic shear zone (Gupta and Bickle 2004). The foliation in the shear zone is shallowly north dipping and the stretching lineation has the same trend as the stretching lineations around pristine and partially chloritized garnet (Fig. 4a, e, f). In garnet-mica schist, garnet is commonly thoroughly chloritized. Shear-band structures and asymmetric folds with axes subparallel to the stretching lineation are common. The shear sense is top-to-the-N (Fig. 6d). Granitic gneiss grades into quartz-feldspar mylonite (Fig. 6e) and metaaplite dikes are rotated into concordance with the mylonitic foliation. In orthogneiss, sericite growth controlled by deformation-assisted breakdown of potassium feldspar defines the mylonitic foliation. Mylonitic deformation results in the development of deformation

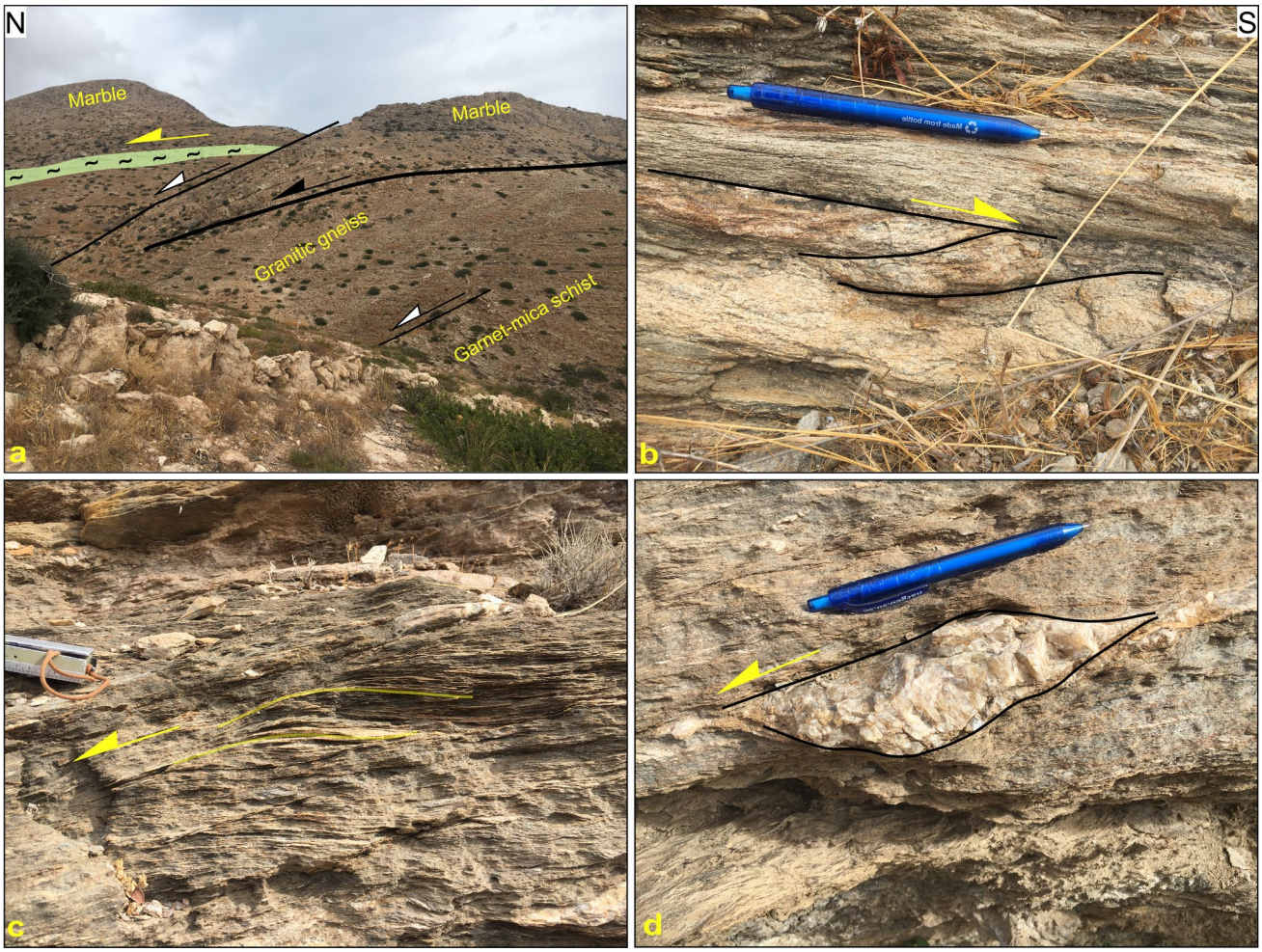


**Fig. 5** Field photographs from the Cycladic basement. **a** Annotated photo of the basement/passive-margin sequence contact at Pantaleimona Bay showing granitic gneiss and garnet-mica schist of the basement tectonically overlain by marble. Two N-dipping normal faults and a top-N shear zone (green) in quartz-chlorite-albite-mica schist are also shown. Note that geographic directions are distorted because of the panoramic image. **b** S-C fabric in felsic metavolcanic rock indicating top-S sense of shear (36°39′36″N, 25°07′17″E). **c** Top-N shear bands in chlorite-mica-albite schist near the base of the passive-margin sequence. **d** Asymmetric quartz boudin in the same rock type as in **c** (photos **c**, **d** near 36°39′52″N, 25°07′16″E)

lamellae in quartz, albite flame growth in potassium feldspar, and pronounced sericitization of plagioclase (Gupta and Bickle 2004). Clinozoisite becomes unstable in asymmetric top-to-the-N structures (Fig. 6f). In metavolcanics, white mica wraps around deformed quartz and microcline porphyroclasts, also indicating a top-to-the-N shear sense.

The actual contact of the Cycladic basement with marble of the passive-margin sequence is characterized by pronounced subgreenschist-facies to cataclastic deformation (Gupta and Bickle 2004; Augier et al. 2015; Ring and Glodny 2021) associated with an N-S-trending stretching lineation (Fig. 4g). In granitic gneiss, low- and high-angle shear bands provide a top-to-the-N shear sense (Fig. 6g, h), although some conflicting kinematic indicators occur as well.

Above the marble at the bottom of the CBU, a 30–40 m thick shear zone developed within lower greenschist-facies quartz-chlorite-albite-mica schist (Fig. 4a, b). Kinematic indicators associated with a subhorizontal, mylonitic foliation provide a consistent top-to-the-N shear sense (Fig. 5c, d).

## Rb–Sr data

Based on microtextural criteria, sample SIK20-16 was selected for Rb–Sr multimineral dating. The sample is a

garnet-mica schist composed of garnet, white mica, quartz, potassium feldspar, plagioclase, albite, chlorite and accessory minerals (Fig. 7a). Some garnet is chloritized along the rims and in strain shadows (Fig. 7b), while in other parts of the thin section garnet is more strongly chloritized. The white-mica fabric contains fine, black interlayers composed of chlorite and quartz-albite aggregates that were mylonitically deformed during top-to-the-S shear (Fig. 6b, c). The Rb–Sr mineral data of the mylonitically deformed minerals date recrystallization and thus fabric formation in this sample (cf. Inger and Cliff 1994; Freeman et al. 1997; Egli et al. 2016).

Regression of Rb–Sr data of three white mica grains-size fractions, apatite and a titanite + zircon concentrate provides a well-defined five-point isochron age of 23.20 ± 0.25 Ma (MSWD = 2.3; 2$\sigma$ errors; Fig. 8). The three white-mica grain-size fractions show a tight cluster. Small white mica grains (200–160 µm grain-size fraction in Fig. 8) growing from feldspar into the strain shadows provide the same apparent ages as larger white mica that wrap around feldspar grains. Therefore, the age of 23.20 ± 0.25 Ma is best interpreted as constraining full recrystallization (isotopic homogenization) of the fabric during ductile mylonitization at lower greenschist-facies metamorphic conditions during top-to-the-S shearing in the Cycladic basement.

## Discussion

### Regional correlations

The footwall of the contact between the basement and passive-margin sequence of the CBU on Sikinos Island is characterized by a ductile-to-brittle top-to-the-N shear zone that structurally upwards shows a distinct subgreenschist-facies to cataclastic overprint. Such a pronounced upward increase in brittle deformation of the footwall is typical for extensional shear zones in the Cyclades (e.g., Lee and Lister 1992; Gautier and Brun 1994; Lister and Forster 1996; Brichau et al. 2006; Bakowsky et al. 2023).

Top-to-the-S shear on Sikinos Island is generally related to thrusting of the passive-margin sequence onto the basement (Gupta and Bickle 2004; Augier et al. 2015). Therefore, Ring and Glodny (2021) speculated that top-to-the-S shearing could be 35–30 Ma in age. Surprisingly, our Rb–Sr age indicates that retrograde, lower greenschist-facies top-to-the-S shear structures formed at 23.20 ± 0.25 Ma. This age coincides with the onset of large-scale horizontal extension in the Cyclades (see reviews in Ring et al. 2010; Grasemann et al. 2012; Glodny and Ring 2022), and also with the inception of top-to-the-S extensional deformation on Folegandros Island (Bakowsky et al. 2023). Furthermore, the age agrees with the onset of sediment deposition in the early extensional basins in the Cyclades (Angelier et al. 1978; Büttner and Kowalczyk 1978; Rösler 1978; Dermitzakis et al. 1980; Böger 1983; Sánchez-Gómez et al. 2002; Kuhlemann et al. 2004). Therefore, we relate the lower greenschist-facies top-to-the-S structures to reflect extensional shearing in the southern Cyclades.

Our well-defined age of 23.20 ± 0.25 Ma from the upper Cycladic basement on Sikinos is indistinguishable from the recently reported $^{40}Ar/^{39}Ar$ ages of ~ 23 Ma for a lower greenschist-facies top-to-the-S extensional shear zone at the contact between the CBU passive-margin sequence and the overlying Pelagonian Unit on Folegandros Island (Bakowsky et al. 2023). These authors showed that the top-to-the-S Folegandros detachment is cutting structurally downward from the Pelagonian/CBU contact to the passive-margin sequence/basement contact (their Fig. 9). This geometry makes it likely that the Folegandros Detachment laterally links up with the top-to-the-S structures at the top of the Cycladic basement on Sikinos, and also with the more localized top-to-the-S South Cyclades Shear Zone/Ios Detachment at the passive-margin sequence/basement contact in South Ios (Fig. 9). Nonetheless, Bakowsky et al. (2023) linked the Folegandros Detachment with the top-to-the-S Thira (Santorini) Detachment and proposed that these two detachments are linked by a large-scale relay structure. Such a scenario demands that the Folegandros Detachment would first cut down structural section (Bakowsky et al. 2023, their Fig. 9) and then cuts up the structural section again in the transport direction to the Pelagonian/CBU passive-margin sequence contact on Thira. We suggest that a correlation of the top-to-the-S extensional detachments on Folegandros and South Ios via the top-to-the-S structures in the Sikinos basement appears to be a geometrically more straightforward solution as in this scenario the extensional detachment would simply cut structurally downwards in the transport direction.

The actual passive-margin sequence/basement contact on Sikinos is a top-to-the-N extensional shear zone. The simplest option for regionally correlating this top-to-the-N shear zone would be to link it with the North Ios Detachment (Fig. 9), which also straddles the passive-margin sequence/basement contact some 30 km further to the east.

Despite our proposition that retrograde, lower greenschist-facies top-to-the-S shearing in the upper Cycladic basement on Sikinos Island resulted from extensional deformation at ~ 23 Ma, the passive-margin sequence/basement contact must have been an earlier thrust that placed the 16–20 kbar passive-margin sequence on top of the 10–12

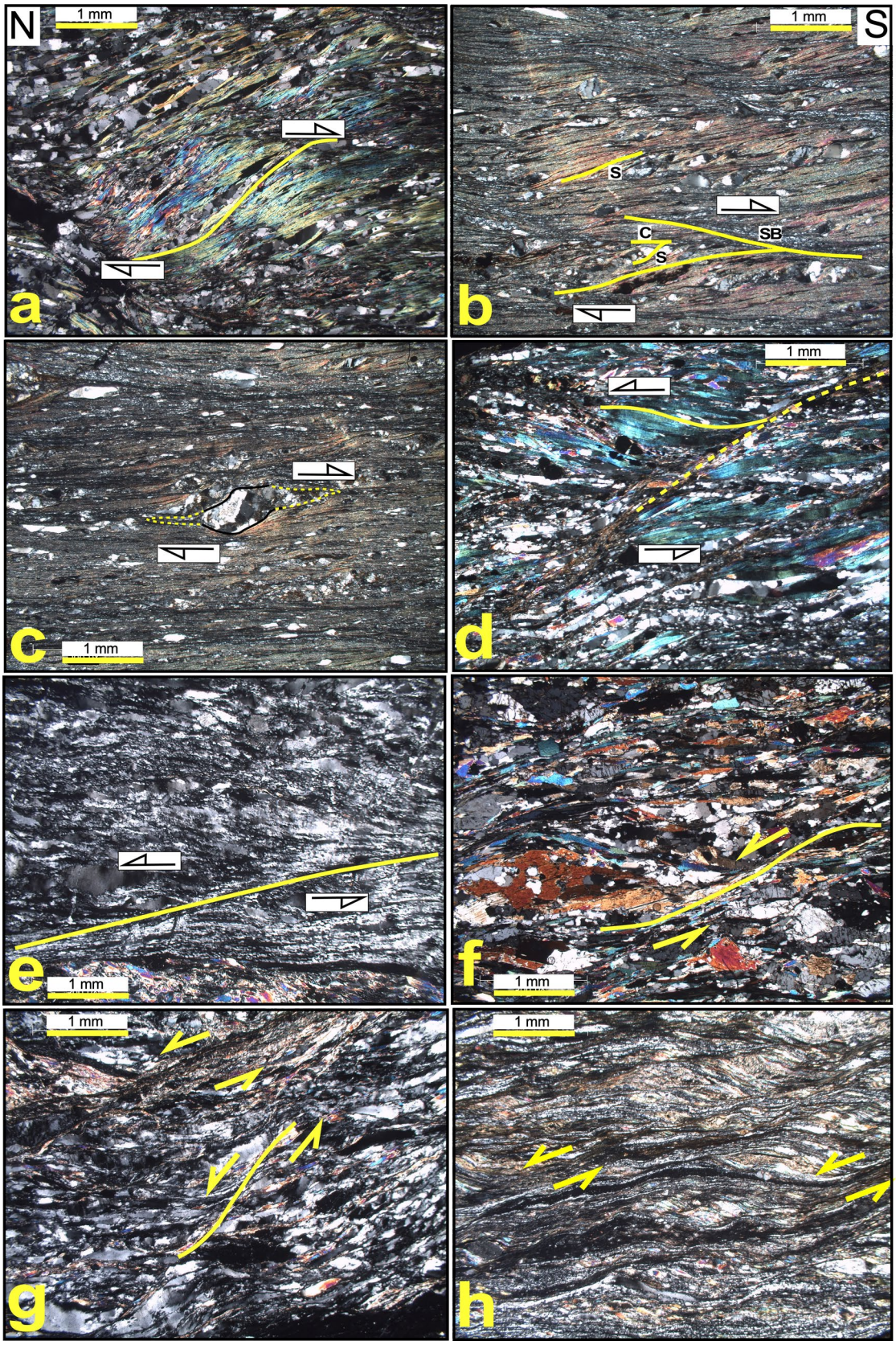
N
1 mm
a
1 mm
S
b
S
C
SB
S
c
1 mm
d
1 mm
e
1 mm
f
1 mm
g
1 mm
h
1 mm

◂**Fig. 6** Microphotographs illustrating top-S and top-N structures in the Cycladic basement. **a** White mica top-S S-C fabric; sample SIK20-17 (36°39′52″N, 25°07′16″E). **b**, **c** Sample SIK20-16 showing sheared white-mica fabric with asymmetric plagioclase and quartz porphyroclasts. White mica recrystallization along S-C planes and also in fine, overprinting shear bands (SB), all structures provide a top-S shear sense. Note that the fine, dark planes along the shear bands and S-C planes are composed of chlorite and very fine-grained, intergrown albite-quartz aggregates (locality of sample see Fig. 4). **d** S-C fabric made up by white mica cut by shear bands (dotted, yellow line) interpreted to reflect continuous top-N shearing during exhumation; sample SIK20-17 (locality see above). **e** Ultramylonitic quartz-feldspar band with top-N shear bands; sample SIK20-4. A few small, new grains around feldspar are interpreted to be due to quartz subgrain rotation recrystallization surrounding the feldspars (36°39′36″N, 27°07′18″E). **f** Top-N shear bands associated with the breakdown of clinozoisite; sample SIK20-5 (36°39′54″N, 27°07′34″E). **g** Same thin section as in **e** showing late, low and high-angle top-N shear bands. **h** Series of top-N shear bands in the direct footwall of subgreenschist-facies to cataclastic rocks at the basement/passive-margin sequence contact; sample SIK24-2 (36°39′41″N, 25°07′45″E)

kbar basement. Either the thrust-related structures are entirely erased, or, probably more likely, there are two sets of top-to-the-S structures with different ages in the Sikinos basement. Our work suggests that upper greenschist-facies top-to-the-S structures are associated with non-chloritized garnet, started to form close to Tertiary peak P–T conditions of 10–12 kbar and 480 ± 20 °C (Franz et al. 1993; Gupta and Bickle 2004) and persisted during isothermal decompression at temperatures > ~ 450 °C (Fig. 4c). The lower greenschist-facies, extensional top-to-the-S structures dated at 23 Ma formed across the Cyclades at temperatures of < ~ 390–350 °C (Kleine et al. 2014) (Fig. 4c). A scenario with two sets of top-to-the-S structures would match the situation in South Ios, where top-to-the-S thrusting (Huet et al. 2009) occurred at 34–32 Ma (Thomson et al. 2009; Forster et al. 2020) followed by retrograde lower greenschist-facies top-to-the-S extensional shearing persisting at least until ~ 18 Ma (Thomson et al. 2009).

### Extensional hinge zone

The top-to-the-S and top-to-the-N extensional structures on the islands of Folegandros, Sikinos and Ios show a bivergent geometry, which Ring and Glodny (2021) considered an extensional hinge zone (Fig. 9). Thomson et al. (2009) and Bakowsky et al. (2023) came to a similar conclusion by arguing that the extensional structures on these three islands are characterized by opposing kinematics and a high degree of coaxial vertical ductile thinning (Mizera and Behrmann 2016). Bakowsky et al. (2023) also argued that coaxial ductile thinning played a significant role in accommodating Miocene extension in the southern Cyclades, corroborating earlier quantitative work by Kumerics et al. (2005), Ring and Kumerics (2008) and Ring and Glodny (2021).

On Sikinos Island, the actual passive-margin sequence/basement contact is a distinct top-to-the-N extensional shear zone. Both the hanging and footwall of the contact are characterized by a component of coaxial deformation as shown by small kinematic vorticity numbers and opposing shear senses (Ring and Glodny 2021). On Folegandros Island, the CBU/Pelagonian Unit contact is a localized top-to-the-S extensional shear zone (Bakowsky et al. 2023). It might be that the contacts between the major units (e.g., the contacts between the passive-margin sequence and the basement as well as the CBU and the Pelagonian Unit) are characterized by more strongly non-coaxial deformation, whereas the less mylonitized rocks in between the major extensional shear zones deform in a more coaxial fashion during large-scale extensional deformation that opened up the Aegean Sea basin.

Whatever the partitioning of extensional deformation is, top-to-the-N and top-to-the-S shearing occurs in close proximity with each other (Fig. 9). In the southern Cyclades, the top-to-the-S shear zones may have been the first to have formed and were overprinted by top-to-the-N extensional structures (Bakowsky et al. 2023; this study). On Ios Island, top-to-the-S and top-to-the-N extension operated in concert at 18 ± 1 Ma (Thomson et al. 2009). At the southern end of the Cyclades (Thira and Anafi islands), the extensional detachments have a monovergent top-to-the-S shear sense (Soukis and Papanikolaou 2004; Schneider et al. 2018; Fig. 9).

At the regional scale, bivergent extension has also been reported from the nearby Menderes Massif in westernmost Anatolia. Gessner et al. (2001, 2013) showed that the late Miocene Kuzey and Güney detachments of the Central Menderes metamorphic core complex (Fig. 1) moved at the same time and formed a large-scale syncline in the extensional hinge zone due to drag in the footwalls of both detachments.

## Conclusions

We showed that top-to-the-S deformation in the Cycladic basement on Sikinos Island occurred at 23.20 ± 0.25 Ma. Our interpretation is that top-to-the-S shearing constraints the onset of extensional deformation in the Cyclades and was overprinted by top-to-the-N extensional structures. This sequence of extensional deformation structures is similar to the geometry of extensional deformation on nearby Folegandros Island. At the regional scale, the geometry of extensional deformation in the southern Cyclades defines an extensional hinge zone.

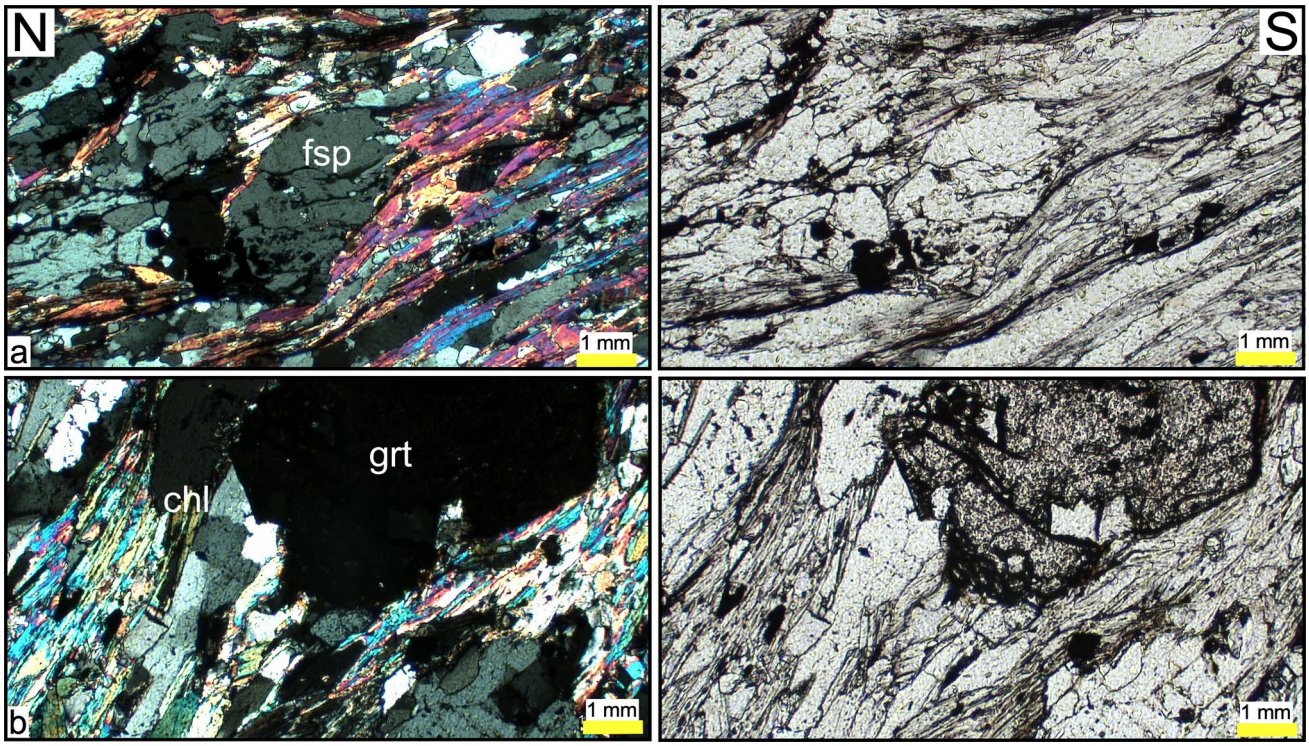


**Fig. 7** Microphotographs of dated sample SIK20-16. Plane-polarized images are on the left and cross-polarized ones on the right. **a** Recrystallized white mica around asymmetric feldspar; top-S sense of shear. **b** Garnet replaced by chlorite, white mica and quartz

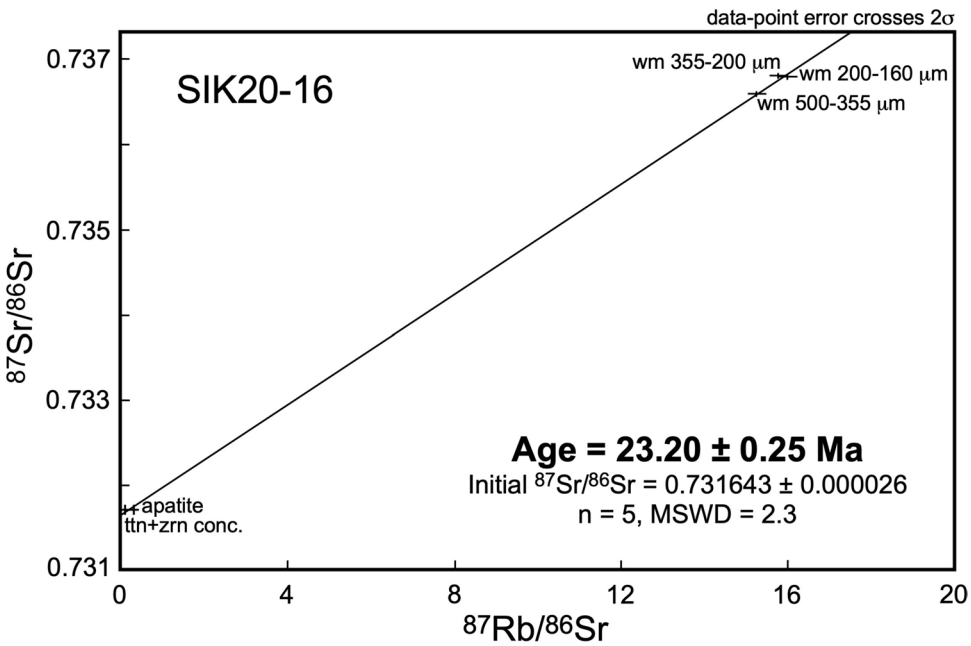


**Fig. 8** Five-point Rb–Sr isochron of sample SIK20-16. The three white-mica grain-size fractions show a tight cluster, which together with apatite and titanite + zircon define an age of 23.20 ± 0.25 Ma

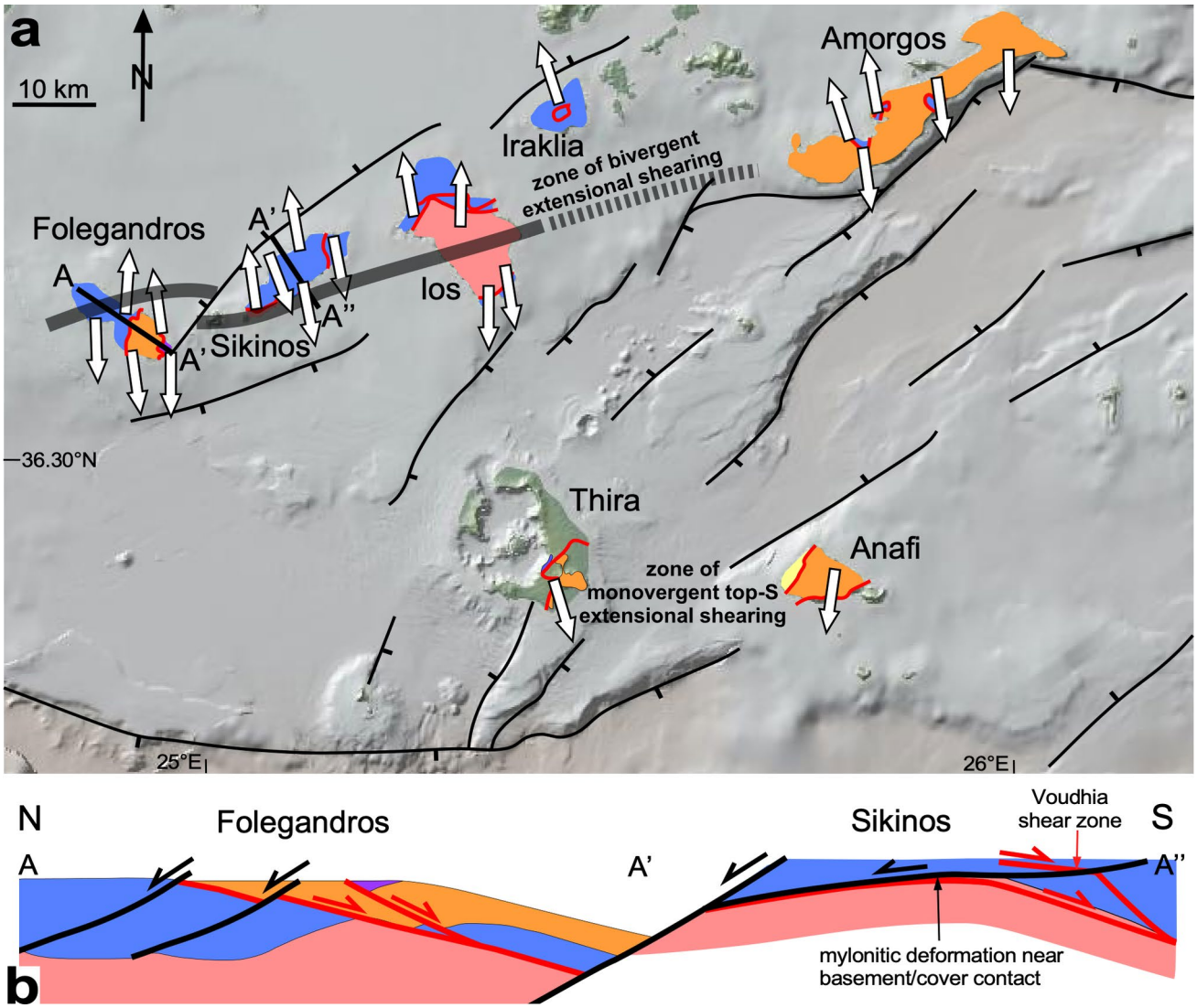


**Fig. 9** **a** Summary of extensional deformation at the south end of the Cyclades. **a** The simplified tectonic map shows top-N and top-S lower- to subgreenschist-facies extensional shear zones on the islands of Folegandros (Bakowsky et al. 2023), Sikinos (Gupta and Bickle 2004; Augier et al. 2015; Ring and Glodny 2021, this study), Ios (Vandenberg and Lister 1996; Huet et al. 2009; Thomson et al. 2009) and Amorgos (Rosenbaum et al. 2007; Ring et al. 2009; Laskari et al. 2024), top-N extension on Iraklia Island (Laskari et al. 2022), and top-S extension on Anafi (Soukis and Papanikolaou 2004) and Thira Island (Schneider et al. 2018). The normal faults are according to Papadimitriou et al. (2015). The dark grey line depicts the zone of a bivergent extensional system characterized by pronounced vertical ductile shortening. **b** Composite cross section (A–A′–A″) (modified from Sowa 1985; Bakowsky et al. 2023) schematically interpreting top-S and top-N extensional structures on the islands of Sikinos and Folegandros

**Supplementary Information** The online version contains supplementary material available at https://doi.org/10.1007/s00531-025-02521-2.

**Acknowledgements** Funded by the Swedish Science Council (Vetenskapsrådet Grant 2021-04075). We thank Gernold Zulauf for a meticulous and Franz Neubauer for a supportive review, as well as Ulrich Riller for editorial handling. Olivier Vanderhaeghe constructively reviewed an earlier version of this manuscript.

**Funding** Open access funding provided by Stockholm University. Openaccess funding provided by Stockholm University.

**Data availability** All data used in this study are available in the manuscript and the Online Resource, which is available at https://doi.org/https://doi.org/10.17045/sthlmuni.27283353.v1.

## References


Altherr R, Kreuzer H, Wendt I, Lenz H, Wagner GA, Keller J, Harre W, Höhndorf A (1982) A late Oligocene/early Miocene high temperature belt in the Attic-Cycladic crystalline complex (SE Pelagonian, Greece). Geophysik 23:97–164

Andriessen PAM, Banga G, Hebeda EH (1987) Isotopic age study of pre-Alpine rocks in the basal units on Naxos, Sikinos and Ios. Greek Cyclades Geol En Mijnb 66:3–14

Angelier J, Glaçon G, Muller C (1978) Sur la présence et la position tectonique du Miocène inférieur marin dans l'archipel de Naxos (Cyclades, Grèce). Comptes Rendus Acad des Sci 286:21–24

Augier R, Jolivet L, Gadenne L, Lahfid A, Driussi O (2015) Exhumation kinematics of the Cycladic Blueschists unit and back-arc extension, insight from the Southern Cyclades (Sikinos and Folegandros Islands, Greece). Tectonics 34:152–185. https://doi.org/10.1002/2014TC003664

Avdis V, Photiades A (1999) Sikinos and Folegandros geological map, scale 1 50,000. Institute of Geology and Mineral Exploration, Athens

Avigad D, Garfunkel Z (1989) Low angle faults underneath and above a blueschist belt—Tinos Island, Cyclades, Greece. Terra Nova 1:182–187

Avigad D, Garfunkel Z (1991) Uplift and exhumation of high-pressure metamorphic terrains: the example of the cycladic blueschist belt (Aegean Sea). Tectonophysics 188:357–372. https://doi.org/10.1016/0040-1951(91)90464-4

Bakowsky C, Schneider DA, Grasemann B, Soukis K (2023) Miocene ductile thinning below the Folegandros Detachment System, Cyclades, Greece. Terra Nova 35:220–229. https://doi.org/10.1111/ter.12646

Beaudoin A, Augier R, Laurent V, Jolivet L, Lahfid A, Bosse V, Arbaret L, Rabillard A, Menant A (2015) The Ikaria high-temperature metamorphic core complex (Cyclades, Greece): Geometry, kinematics and thermal structure. J Geodyn 92:18–41. https://doi.org/10.1016/j.jog.2015.09.004

Böger H (1983) Stratigraphische und tektonische Verknüpfungen kontinentaler Sedimente des Neogens im Ägäis-Raum. Geol Rundschau 72:771–813. https://doi.org/10.1007/BF01848344

Bolhar R, Ring U, Allen CM (2010) An integrated zircon geochronological and geochemical investigation into the Miocene plutonic evolution of the Cyclades, Aegean Sea, Greece: Part 1: Geochronology. Contrib Miner Petrol 160:719–742. https://doi.org/10.1007/s00410-010-0504-4

Bolhar R, Ring U, Kemp AIS, Whitehouse MJ, Weaver SD, Woodhead JD, Uysal IT, Turnbull R (2012) An integrated zircon geochronological and geochemical investigation into the Miocene plutonic evolution of the Cyclades, Aegean Sea, Greece: Part 2: Geochemistry. Contrib Miner Petrol 164:915–933. https://doi.org/10.1007/s00410-012-0759-z

Bolhar R, Ring U, Ireland TR (2017) Zircon in amphibolites from Naxos, Aegean Sea, Greece: origin, significance and tectonic setting. J Metamorph Geol 35:413–434. https://doi.org/10.1111/jmg.12238

Brichau S, Ring U, Ketcham RA, Carter A, Stockli D, Brunel M (2006) Constraining the long-term evolution of the slip rate for a major extensional fault system in the central Aegean, Greece, using thermochronology. Earth Planet Sci Lett 241:293–306. https://doi.org/10.1016/j.epsl.2005.09.065

Brichau S, Ring U, Carter A, Monié P, Bolhar R, Stockli D, Brunel M (2007) Extensional faulting on Tinos Island, Aegean Sea, Greece: how many detachments? Tectonics 26:1–19. https://doi.org/10.1029/2006TC001969

Brichau S, Thomson S, Ring U (2010) Thermochronometric constraints on the tectonic evolution of the serifos detachment, Aegean Sea, Greece. Int J Earth Sci 99:379–393. https://doi.org/10.1007/s00531-008-0386-0

Bröcker M, Kreuzer H, Matthews A, Okrusch M (1993) 40Ar/39Ar and oxygen isotope studies of polymetamorphism from Tinos Island, Cycladic blueschist belt, Greece. J Metamorph Geol 11:223–240. https://doi.org/10.1111/j.1525-1314.1993.tb00144.x

Bröcker M, Baldwin S, Arkudas R (2013) The geological significance of 40Ar/39Ar and Rb–Sr white mica ages from Syros and Sifnos, Greece: a record of continuous (re)crystallization during exhumation? J Metamorph Geol 31:629–646. https://doi.org/10.1111/jmg.12037

Bröcker M, Löwen K, Rodionov N (2014) Unraveling protolith ages of meta-gabbros from Samos and the Attic-Cycladic Crystalline Belt, Greece: results of a U–Pb zircon and Sr–Nd whole rock study. Lithos 198–199:234–248. https://doi.org/10.1016/j.lithos.2014.03.029

Büttner D, Kowalczyk G, (1978) Late Cenozoic stratigraphy and paleogeography of Greece—a review. In: Cloos H et al (ed) Alps, Apennines, Hellenides. Geodynamic investigations along geotraverses by an international group of geoscientists. Schweizerbart, Stuttgart, pp 494–501

Cao S, Neubauer F, Bernroider M, Genser J, Liu J, Friedl G (2017) Low-grade retrogression of a high-temperature metamorphic core complex: Naxos, Cyclades, Greece. Bull Geol Soc Am 129:93–117. https://doi.org/10.1130/B31502.1

Cliff RA, Bond CE, Butler RWH, Dixon JE (2017) Geochronological challenges posed by continuously developing tectonometamorphic systems: insights from Rb–Sr mica ages from the Cycladic Blueschist Belt, Syros (Greece). J Metamorph Geol 35:197–211. https://doi.org/10.1111/jmg.12228

Coleman MJ, Schneider DA, Grasemann B, Soukis K, Lozios S, Hollinetz MS (2020) Lateral termination of a Cycladic-style detachment system (Hymittos, Greece). Tectonics 39:e2020TC006128. https://doi.org/10.1029/2020TC006128

Dermitzakis M, Papanikolaou D, Theodoridis S, Mirkou R (1980) The Molasse of Paros Island, Aegean Sea. Ann Naturhistorischen Museums Wien 83:59–71

Ducharme TA, Schneider DA, Grasemann B, Klonowska I (2022) Stretched thin: Oligocene Extrusion and ductile thinning of the Basal Unit along the Evia Shear Zone, NW Cyclades. Tectonics. https://doi.org/10.1029/2022TC007561

Dürr S (1978) The median Aegean crystalline belt: stratigraphy, structure, metamorphism, magmatism. In: Closs H et al (eds) Alps, Apeninnes, Hellenides. Schweizerbart, Stuttgart, pp 537–564

Egli D, Müller W, Mancktelow N (2016) Laser-cut Rb–Sr microsampling dating of deformational events in the Mont Blanc-Aiguilles Rouges region (European Alps). Terra Nova 28:35–42. https://doi.org/10.1111/ter.12184

Flansburg ME, Stockli DF, Poulaki EM, Soukis K (2019) Tectonomagmatic and stratigraphic evolution of the Cycladic Basement, Ios Island, Greece. Tectonics 38:2291–2316. https://doi.org/10.1029/2018TC005436

Forster M, Koudashev O, Nie R, Yeung S, Lister G (2020) 40Ar/39Ar thermochronology in the Ios basement terrane resolves the tectonic significance of the South Cyclades Shear Zone. Geol Soc Spec Publ 487:291–313. https://doi.org/10.1144/SP487-2018-169

Franz BL, Okrusch M, Bröcker M (1993) Polymetamorphic evolution of pre-Alpidic basement rocks on the island of Sikinos (Cyclades,

Greece). Neues Jahrb Für Miner 4:145–162. https://doi.org/10.1127/0077-7757/2005/0013
Freeman SR, Inger S, Butler RWH, Cliff RA (1997) Dating deformation using Rb–Sr in white mica: Greenschist facies deformation ages from the Entrelor shear zone, Italian Alps. Tectonics 16:57–76. https://doi.org/10.1029/96TC02477
Gautier P, Brun J-P (1994) Ductile crust exhumation and extensional detachments in the central Aegean (Cyclades and Evvia Islands). Geodin Acta 7:57–85. https://doi.org/10.1080/09853111.1994.11105259
Gessner K, Ring U, Johnson C, Hetzel R, Passchier CW, Güngör T (2001) An active bivergent rolling-hinge detachment system: Central Menderes metamorphic core complex in western Turkey. Geology 29:611–614. https://doi.org/10.1130/0091-7613(2001)029%3c0611:AABRHD%3e2.0.CO;2
Gessner K, Gallardo LA, Markwitz V, Ring U, Thomson SN (2013) What caused the denudation of the Menderes Massif: review of crustal evolution, lithosphere structure, and dynamic topography in southwest Turkey. Gondwana Res 24:243–274. https://doi.org/10.1016/j.gr.2013.01.005
Glodny J, Ring U (2022) The Cycladic Blueschist Unit of the Hellenic subduction orogen: protracted high-pressure metamorphism, decompression and reimbrication of a diachronous nappe stack. Earth Sci Rev. https://doi.org/10.1016/j.earscirev.2021.103883
Glodny J, Kühn A, Austrheim H (2008a) Diffusion versus recrystallization processes in Rb–Sr geochronology: isotopic relics in eclogite facies rocks, Western Gneiss Region, Norway. Geochim Cosmochim Acta 72:506–525. https://doi.org/10.1016/j.gca.2007.10.021
Glodny J, Ring U, Kühn A (2008b) Coeval high-pressure metamorphism, thrusting, strike-slip, and extensional shearing in the Tauern Window, Eastern Alps. Tectonics. https://doi.org/10.1029/2007TC002193
Grasemann B, Schneider DA, Stöckli DF, Iglseder C (2012) Miocene bivergent crustal extension in the Aegean: evidence from the western Cyclades (Greece). Lithosphere 4:23–39. https://doi.org/10.1130/L164.1
Grütter HS (1993) Structural and metamorphic studies on Ios, Cyclades, Greece. PhD Thesis, University of Cambridge
Gupta S, Bickle MJ (2004) Ductile shearing, hydrous fluid channelling and high-pressure metamorphism along the basement-cover contact on Sikinos, Cyclades, Greece. Geol Soc Spec Publ 224:161–175. https://doi.org/10.1144/GSL.SP.2004.224.01.11
Huet B, Labrousse L, Jolivet L (2009) Thrust or detachment? exhumation processes in the aegean: insight from a field study on ios (Cyclades, Greece). Tectonics 28:1–27. https://doi.org/10.1029/2008TC002397
Inger S, Cliff RA (1994) Timing of metamorphism in the Tauern Window, Eastern Alps: Rb–Sr ages and fabric formation. J Metamorph Geol 12:695–707. https://doi.org/10.1111/j.1525-1314.1994.tb00052.x
Jacobshagen V, Dürr S, Kockel F, Makris J, Meyer W, Röwer P, Schröder B, Seidel E, Wachendorf H, Dornsiepen U, Giese P, Wallbrecher E (1986) Geologie von Griechland, vol 19. Berträge zur Reg. Geol. der Erde. Borntraeger, Berlin
Jolivet L, Brun JP (2010) Cenozoic geodynamic evolution of the Aegean. Int J Earth Sci 99:109–138. https://doi.org/10.1007/s00531-008-0366-4
Jolivet L, Lecomte E, Huet B, Denèle Y, Lacombe O, Labrousse L, Le Pourhiet L, Mehl C (2010) The North Cycladic detachment system. Earth Planet Sci Lett 289:87–104. https://doi.org/10.1016/j.epsl.2009.10.032
Jolivet L, Menant A, Sternai P, Rabillard A, Arbaret L, Augier R, Laurent V, Beaudoin A, Grasemann B, Huet B, Labrousse L, Le Pourhiet L (2015) The geological signature of a slab tear below the Aegean. Tectonophysics 659:166–182. https://doi.org/10.1016/j.tecto.2015.08.004
Kleine BI, Skelton ADL, Huet B, Pitcairn IK (2014) Preservation of Blueschist-facies minerals along a Shear Zone by Coupled Metasomatism and Fast-flowing $CO_2$-bearing fluids. J Petrol 55:1905–1939. https://doi.org/10.1093/petrology/egu045
Kuhlemann J, Frisch W, Dunkl I, Kázmér M, Schmiedl G (2004) Miocene siliciclastic deposits of Naxos Island: geodynamic and environmental implications for the evolution of the southern Aegean Sea (Greece). Spec Pap Geol Soc Am 378:51–65. https://doi.org/10.1130/0-8137-2378-7.51
Kumerics C, Ring U, Brichau S, Glodny J, Monié P (2005) The extensional Messaria shear zone and associated brittle detachment faults, Aegean Sea, Greece. J Geol Soc 162:701–721
Lamont TN, Roberts NM, Searle MP, Gardiner NJ, Gopon P, Hsieh YT, Holdship P, White RW (2023)Contemporaneous crust-derived I-and S-type granite magmatism and normal faulting on Tinos, Delos, and Naxos, Greece:Constraints on Aegean orogenic collapse. Bull Geol Soc. Am 135(11–12):2797–2829
Laskari S, Soukis K, Lozios S, Stockli DF, Poulaki EM, Stouraiti C (2022) Structural study and Detrital Zircon Provenance analysis of the Cycladic Blueschist Unit rocks from Iraklia Island: from the Paleozoic basement unroofing to the Cenozoic exhumation. Minerals. https://doi.org/10.3390/min12010083
Laskari S, Soukis K, Lozios S, Stockli DF (2024) Switching from the top-NW backthrusting to top-SE post-orogenic deformation in the Aegean domain: Insights from the calcite microfabric and siliciclastic rocks of the Amorgos Unit (SE Cyclades, Greece). J Struct Geol. https://doi.org/10.1016/j.jsg.2023.105011
Laurent V, Lanari P, Naïr I, Augier R, Lahfid A, Jolivet L (2018) Exhumation of eclogite and blueschist (Cyclades, Greece): pressure–temperature evolution determined by thermobarometry and garnet equilibrium modelling. J Metamorph Geol 36:769–798. https://doi.org/10.1111/jmg.12309
Lee J, Lister GS (1992) Late Miocene ductile extension and detachment faulting, Mykonos, Greece. Geology 20:121–124. https://doi.org/10.1130/0091-7613(1992)020%3c0121:LMDEAD%3e2.3.CO;2
Lister GS, Forster MA (1996) Inside the Aegean metamorphic core complexes: a field trip guide illustrating the geology of . Journal of the Virtual Explorer, 27, paper 1 , 27:41–46. https://doi.org/10.3809/doi
Lister GS, Davis GA (1989) The origin of metamorphic core complexes and detachment faults formed during Tertiary continental extension in the northern Colorado River region, U.S.A. J Struct Geol 11:65–94. https://doi.org/10.1016/0191-8141(89)90036-9
Martin L, Duchêne S, Deloule E, Vanderhaeghe O (2006) The isotopic composition of zircon and garnet: a record of the metamorphic history of Naxos, Greece. Lithos 87:174–192. https://doi.org/10.1016/j.lithos.2005.06.016
Mizera M, Behrmann JH (2016) Strain and flow in the metamorphic core complex of Ios Island (Cyclades, Greece). Int J Earth Sci 105:2097–2110. https://doi.org/10.1007/s00531-015-1259-y
Okrusch M, Bröcker M (1990) Eclogites associated with high-grade blueschists in the Cyclades archipelago, Greece: a review. Eur J Mineral 2:451–478. https://doi.org/10.1127/ejm/2/4/0451
Papadimitriou P, Kapetanidis V, Karakonstantis A, Kaviris G, Voulgaris N, Makropoulos K (2015) The Santorini Volcanic Complex: a detailed multi-parameter seismological approach with emphasis on the 2011–2012 unrest period. J Geodyn 85:32–57. https://doi.org/10.1016/j.jog.2014.12.004
Peillod A, Ring U, Glodny J, Skelton A (2017) An Eocene/Oligocene blueschist-/greenschist facies P-T loop from the Cycladic Blueschist Unit on Naxos Island, Greece: deformation-related re-equilibration vs. thermal relaxation. J Metamorph Geol 35:805–830. https://doi.org/10.1111/jmg.12256
Peillod A, Majka J, Ring U, Drüppel K, Patten C, Karlsson A, Włodek A, Tehler E (2021a) Differences in decompression of

a high-pressure unit: a case study from the Cycladic Blueschist Unit on Naxos Island, Greece. Lithos. https://doi.org/10.1016/j.lithos.2021.106043

Peillod A, Tehler E, Ring U (2021b) Quo vadis Zeus: is there a Zas shear zone on Naxos Island, Aegean Sea, Greece? A review of metamorphic history and new kinematic data. J Geol Soc Lond 178:jgs2020-217. https://doi.org/10.1144/jgs2020-217

Peillod A, Patten CGC, Drüppel K, Beranoaguirre A, Zeh A, Gudelius D, Hector S, Majka J, Kleine-Marshall BI, Karlson A, Gerdes A, Kolb J (2024) Disruption of a high-pressure unit during exhumation: example of the Cycladic Blueschist unit (Thera, Ios and Naxos islands, Greece). J Metamorph Geol 42:225–255. https://doi.org/10.1111/jmg.12753

Poulaki EM, Stockli DF, Flansburg ME, Soukis K (2019) Zircon U–Pb chronostratigraphy and provenance of the Cycladic Blueschist Unit and the nature of the contact with the Cycladic Basement on Sikinos and Ios Islands, Greece. Tectonics 38:3586–3613. https://doi.org/10.1029/2018TC005403

Pryer LL (1993) Microstructures in feldspars from a major crustal thrust zone: the Grenville Front, Ontario, Canada. J Struct Geol 15:21–36. https://doi.org/10.1016/0191-8141(93)90076-M

Reischmann T (1998) Pre-Alpine origin of tectonic units from the metamorphic complex of Naxos, Greece, identified by single zircon Pb/Pb dating. Bull Geol Soc Greece XXXII/3:101–111

Ring U, Glodny J (2021) Geometry and kinematics of Bivergent Extension in the Southern Cycladic Archipelago: constraining an extensional hinge zone on Sikinos Island, Aegean Sea, Greece. Tectonics 40:1–24. https://doi.org/10.1029/2020TC006641

Ring U, Kumerics C (2008) Vertical ductile thinning and its contribution to the exhumation of high-pressure rocks: the Cycladic blueschist unit in the Aegean. J Geol Soc Lond 165:1019–1030. https://doi.org/10.1144/0016-76492008-010

Ring U, Layer PW (2003) High-pressure metamorphism in the Aegean, eastern Mediterranean: underplating and exhumation from the Late Cretaceous until the Miocene to Recent above the retreating Hellenic subduction zone. Tectonics 22(3):1022. https://doi.org/10.1029/2001TC001350

Ring U, Laws S, Bernet M (1999) Structural analysis of a complex nappe sequence and late-orogenic basins from the Aegean Island of Samos, Greece. J Struct Geol 21:1575–1601. https://doi.org/10.1016/S0191-8141(99)00108-X

Ring U, Thomson SN, Bröcker M (2003) Fast extension but little exhumation: the Vari detachment in the Cyclades, Greece. Geol Mag 140:245–252. https://doi.org/10.1017/S0016756803007799

Ring U, Thomson SN, Rosenbaum G (2009) Timing of the Amorgos detachment system and implications for detachment faulting in the southern Aegean Sea, Greece. Geol Soc Spec Publ 321:169–178. https://doi.org/10.1144/SP321.8

Ring U, Glodny J, Will T, Thomson S (2010) The Hellenic subduction system: high-pressure metamorphism, exhumation, normal faulting, and large-scale extension. Annu Rev Earth Planet Sci 38:45–76. https://doi.org/10.1146/annurev.earth.050708.170910

Ring U, Glodny J, Will TM, Thomson S (2011) Normal faulting on Sifnos and the south Cycladic detachment system, Aegean sea, Greece. J Geol Soc Lond 168:751–768. https://doi.org/10.1144/0016-76492010-064

Ring U, Glodny J, Peillod A, Skelton A (2018) The timing of high-temperature conditions and ductile shearing in the footwall of the Naxos extensional fault system, Aegean Sea, Greece. Tectonophysics 745:366–381. https://doi.org/10.1016/j.tecto.2018.09.001

Rosenbaum G, Ring U, Kühn A (2007) Tectonometamorphic evolution of high-pressure rocks from the island of Amorgos (Central Aegean, Greece). J Geol Soc Lond 164:425–438. https://doi.org/10.1144/0016-76492006-005

Rösler G (1978) Relics of non-metamorphic sediments on central Aegean Islands. In: Closs H, Roeder D, Schmidt K (eds) Alps, Apennines, Hellenides, vol 38. Inter-Union Commission on Geodynamics Scientific Report. E. Schweizerbart, Stuttgart, pp 480–481

Ryan WBF, Carbotte S, Coplan JO, O'Hara S, Melkonian A, Arko R, Weissel RA, Ferrini V, Goodwillie A, Nitsche F, Bonczkowski J, Zemsky R (2009) Global multi-resolution topography synthesis. Geochem Geophys Geosyst. https://doi.org/10.1029/2008GC002332

Sánchez-Gómez M, Avigad D, Heimann A (2002) Geochronology of clasts in allochthonous Miocene sedimentary sequences on Mykonos and Paros Islands: implications for back-arc extension in the Aegean Sea. J Geol Soc Lond 159:45–60. https://doi.org/10.1144/0016-764901031

Scheffer C, Vanderhaeghe O, Lanari P, Tarantola A, Ponthus L, Photiades A, France L (2016) Syn- to post-orogenic exhumation of metamorphic nappes: Structure and thermobarometry of the western Attic-Cycladic metamorphic complex (Lavrion, Greece). J Geodyn 96:174–193. https://doi.org/10.1016/j.jog.2015.08.005

Schneider DA, Grasemann B, Lion A, Soukis K, Draganits E (2018) Geodynamic significance of the Santorini Detachment System (Cyclades, Greece). Terra Nova 30:414–422. https://doi.org/10.1111/ter.12357

Soukis K, Papanikolaou D (2004) Contrasting geometry between Alpine and late- to post-Alpine tectonic structures in Anafi Island (Cyclades). Bull Geol Soc Greece 36:1688–1696. https://doi.org/10.12681/bgsg.16575

Sowa A (1985) Die Geologie des Insel Folegandros (Kykladen, Griechenland). Erlanger Geol Abh 112:85–101

Thomson SN, Ring U, Brichau S, Glodny J, Will TM (2009) Timing and nature of formation of the Ios metamorphic core complex, southern Cyclades, Greece. Geol Soc Spec Publ 321:139–167. https://doi.org/10.1144/SP321.7

van der Maar P (1981) Metamorphism on Ios and the geological history of the Southern Cyclades, Greece. Geol Ultraiectina 28:1–142

van der Maar PA, Jansen JBH (1983) The geology of the polymetamorphic complex of Ios, Cyclades, Greece and its significance for the Cycladic Massif. Geol Rundsch 72:283–299. https://doi.org/10.1007/BF01765910

Vandenberg LC, Lister GS (1996) Structural analysis of basement tectonites from the Aegean metamorphic core complex of Ios, Cyclades, Greece. J Struct Geol 18:1437–1454. https://doi.org/10.1016/S0191-8141(96)00068-5

Vanderhaeghe O (2004) Structural development of the Naxos migmatite dome. Spec Pap Geol Soc Am 380:211–227. https://doi.org/10.1130/0-8137-2380-9.211

Vanderhaeghe O, Hibsch C, Siebenaller L, Martin L, Duchêne S, de St Blanquat M, Kruckenberg S, Fotiadis A (2007) Penrose conference—extending a continent—Naxos Field guide. J Virtual Explor. https://doi.org/10.3809/jvirtex.2007.00175

Wijbrans JR, McDougall I (1988) Metamorphic evolution of the Attic Cycladic Metamorphic Belt on Naxos (Cyclades, Greece) utilizing 40Ar/39Ar age spectrum measurements. J Metamorph Geol 6:571–594